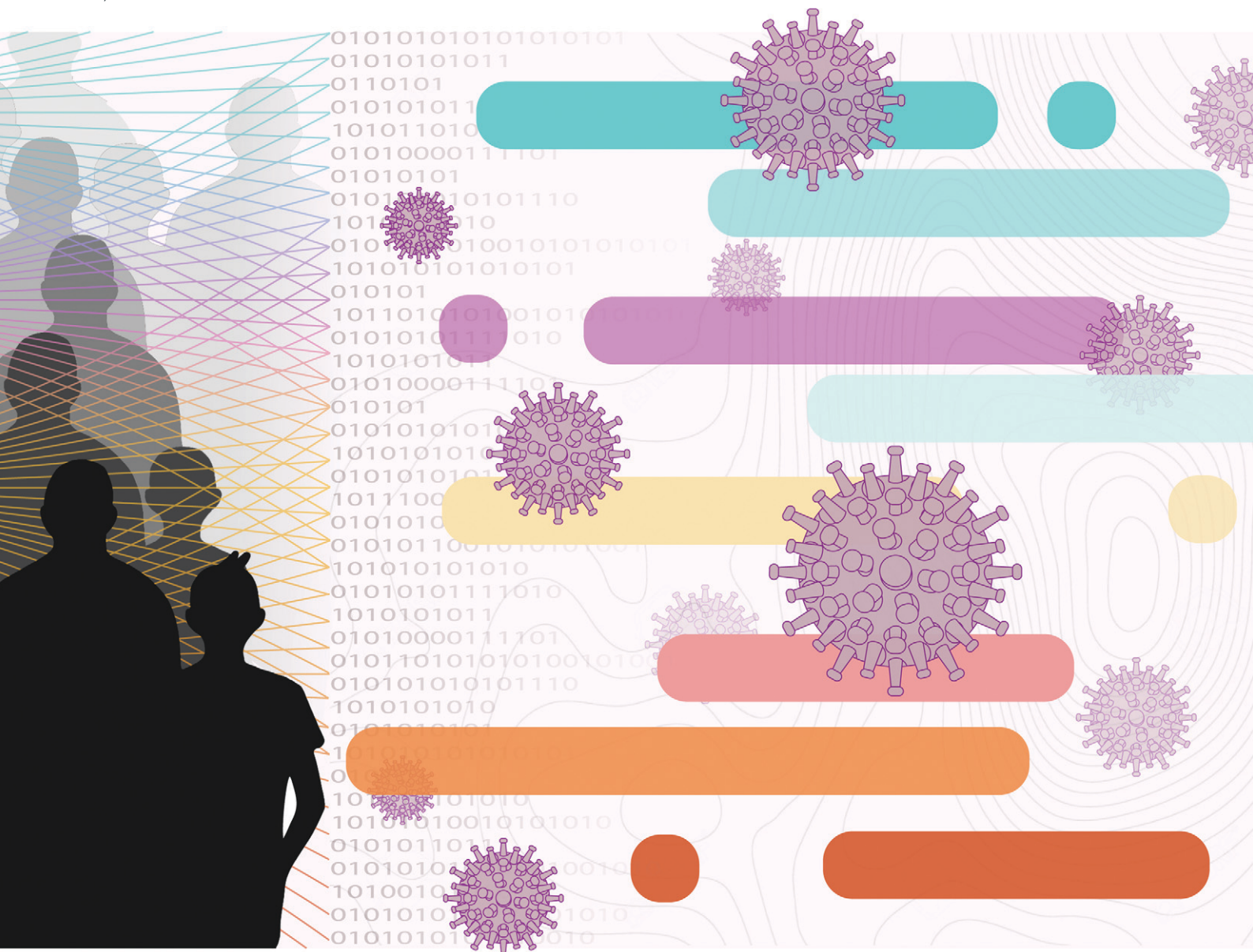


# Environmental Science Water Research & Technology

Volume 8  
Number 7  
July 2022  
Pages 1315–1580

rsc.li/es-water



ISSN 2053-1400

## PAPER

Fangqiong Ling *et al.*  
Emerging investigator series: meta-analyses on SARS-CoV-2  
viral RNA levels in wastewater and their correlations to  
epidemiological indicators

## PAPER

View Article Online  
View Journal | View Issue



Cite this: *Environ. Sci.: Water Res. Technol.*, 2022, **8**, 1391

# Emerging investigator series: meta-analyses on SARS-CoV-2 viral RNA levels in wastewater and their correlations to epidemiological indicators†

David Mantilla-Calderon,<sup>a</sup> Kaiyu (Kevin) Huang,<sup>a</sup> Aojie Li,<sup>a</sup> Kaseba Chibwe,<sup>a</sup> Xiaoqian Yu,<sup>b</sup> Yinyin Ye,<sup>c</sup> Lei Liu<sup>d</sup> and Fangqiong Ling<sup>e</sup>  <sup>\*aefg</sup>

**Background:** recent applications of wastewater-based epidemiology (WBE) have demonstrated its ability to track the spread and dynamics of COVID-19 at the community level. Despite the growing body of research, quantitative synthesis of SARS-CoV-2 RNA levels in wastewater generated from studies across space and time using diverse methods has not been performed. **Objective:** the objective of this study is to examine the correlations between SARS-CoV-2 RNA levels in wastewater and epidemiological indicators across studies, stratified by key covariates in study methodologies. In addition, we examined the association of proportions of positive detections in wastewater samples and methodological covariates. **Methods:** we systematically searched the Web of Science for studies published by February 16th, 2021, performed a reproducible screening, and employed mixed-effects models to estimate the levels of SARS-CoV-2 viral RNA quantities in wastewater samples and their correlations to the case prevalence, the sampling mode (grab or composite sampling), and the wastewater fraction analyzed (i.e., solids, solid-supernatant mixtures, or supernatants/filtrates). **Results:** a hundred and one studies were found; twenty studies (671 biosamples and 1751 observations) were retained following a reproducible screening. The mean positivity across all studies was 0.68 (95%-CI, [0.52; 0.85]). The mean viral RNA abundance was 5244 marker copies per mL (95%-CI, [0; 16 432]). The Pearson correlation coefficients between the viral RNA levels and case prevalence were 0.28 (95%-CI, [0.01; 0.51]) for daily new cases or 0.29 (95%-CI, [-0.15; 0.73]) for cumulative cases. The fraction analyzed accounted for 12.4% of the variability in the percentage of positive detections, followed by the case prevalence (9.3% by daily new cases and 5.9% by cumulative cases) and sampling mode (0.6%). Among observations with positive detections, the fraction analyzed accounted for 56.0% of the variability in viral RNA levels, followed by the sampling mode (6.9%) and case prevalence (0.9% by daily

Received 30th January 2022,  
Accepted 4th May 2022

DOI: 10.1039/d2ew00084a

rscl.li/es-water

## Water impact

Recent applications of wastewater-based epidemiology (WBE) have demonstrated its ability to track the spread and dynamics of COVID-19 at the community level. Despite the growing body of research, quantitative synthesis of SARS-CoV-2 viral RNA levels in wastewater generated from studies across space and time using diverse methods has not been performed. The meta-analysis methodology treats individual studies as members of a population of studies that all provide information on a given effect instead of drawing conclusions on exemplary studies that have shown strong positive effects. Leveraging a large sample size, meta-analysis can help move the narrative beyond statistical significance and draw attention to the magnitude, direction, and variance in effects. This study employed a meta-analysis methodology to quantitatively synthesize results among WBE studies in the first year of the COVID-19 pandemic. Positive pooled means and confidence intervals in the Pearson correlation coefficients between the SARS-CoV-2 viral RNA levels and case prevalence indicators provide quantitative evidence reinforcing the value of wastewater-based monitoring of COVID-19. Large heterogeneities among studies suggest a strong demand for experimental and computational methods to address cross-study heterogeneities. Mixed-effects models accounting for study level variations provide a new perspective to synthesize data from multiple WBE studies.

<sup>a</sup> Department of Energy, Environmental and Chemical Engineering, Washington University in St. Louis, St. Louis, MO, USA. E-mail: fangqiong@wustl.edu

<sup>b</sup> Centre for Microbiology and Environmental Systems Science, Department of Microbiology and Ecosystem Science, Division of Microbial Ecology, University of Vienna, Vienna, Austria

<sup>c</sup> Department of Civil, Structural and Environmental Engineering, University at Buffalo, Buffalo, NY, USA

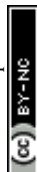
<sup>d</sup> Division of Biostatistics, Washington University in St. Louis, St. Louis, MO, USA

<sup>e</sup> Department of Computer Science and Engineering, Washington University in St. Louis, St. Louis, MO, USA

<sup>f</sup> Division of Biological and Biomedical Sciences, Washington University in St. Louis, St. Louis, MO, USA

<sup>g</sup> Division of Computational and Data Science, Washington University in St. Louis, St. Louis, MO, USA

† Electronic supplementary information (ESI) available. See DOI: <https://doi.org/10.1039/d2ew00084a>



## 1. Introduction

shown strong positive effects, meta-analyses treat individual studies as members of a population of studies that conjunctively provide information on a given effect.<sup>25</sup> Leveraging a large sample size, a meta-analysis can help move the narrative beyond statistical significance and draw attention to the magnitude, direction, and variance in effects.<sup>24</sup> Furthermore, the meta-analytic approach allows us to quantitatively examine the heterogeneity among study results, thus motivating the generation of new hypotheses.<sup>26</sup> Meta-analyses systematically synthesize large quantities of data generated from multiple primary studies to reach broad generalizations. A well-conducted meta-analysis can provide a comprehensive picture of parameters of interest and their moderators that is not attainable from an individual primary study. Using statistical models to quantify the magnitude of an effect and its heterogeneity, a meta-analysis may also identify areas that require further research.

Here, we employed a meta-analytic methodology to synthesize wastewater-based SARS-CoV-2 viral RNA abundance data published by February 16th, 2021, approximately a year after the beginning of the COVID-19 pandemic. Following a PRISMA guideline,<sup>27</sup> we synthesized and reported results from 1751 observations in 20 studies. We asked four fundamental questions: 1) what is the pooled proportion of positive detection of SARS-CoV-2 from wastewater samples; 2) what are the viral RNA levels of the SARS-CoV-2 virus in wastewater collectively and when subgrouped by key methodological variables; 3) what are the overall strengths of correlation between the positive detection or RNA levels of SARS-CoV-2 in wastewater and epidemiological indicators (daily and cumulative cases); and 4) how much of the variation in SARS-CoV-2 viral RNA abundance can be explained by COVID-19 cases alone? To account for study-level variations, mixed-effects models were employed to examine the correlation between SARS-CoV-2 viral RNA levels and positive detection.

## 2. Methods

Results from this systematic review and subsequent meta-analysis have been reported following the PRISMA guidelines.<sup>27</sup> A PRISMA checklist is presented in Table S1.†

## 2.1 Data sources

We searched the Web of Science (WoS) for publications analyzing untreated wastewater for the presence of the SARS-CoV-2 virus published by February 16th, 2021. Studies were retrieved with the search terms: TS = (SARS-CoV-2 AND (wastewater OR sewage)) from the WoS core collection. Including the keyword “COVID-19” in the search terms did not increase the number of resulting records. The following search conditions were applied: i) language was restricted to English; ii) the time span was set to “All Years”; iii) records in the Science Citation Index Expanded (SCI-Expanded) were included; and iv) the document type was set to “article”, “early access” or “letter” to retain original research (*i.e.*, “reviews” or “editorial materials” were not selected).

## 2.2 Study selection and eligibility criteria

Upon study retrieval from the Web of Science, duplication of records was screened by titles and authors. No duplication was found. Next, full-text records were scanned to assess for eligibility. Studies that reported nucleic-acid detections of SARS-CoV-2 from wastewater systems and associated epidemiological indicators were included. Specifically, the following inclusion criteria were applied: 1) original qPCR data in terms of SARS-CoV-2 measurements in wastewater were reported, and data were reported as quantification cycles, copy numbers per volume, genome equivalents per volume, and/or genome equivalents per weight of sample; 2) sampling locations were identified as wastewater treatment plants (WWTPs), sewage collection networks, lift stations, manholes or septic tanks; 3) SARS-CoV-2 case incidence/prevalence is reported for the associated locations during the sampling times. Rationales for each inclusion criterion are provided in Table 1. The study eligibility was assessed by David Mantilla-Calderon (DMC), Kevin Huang (KH), Aojie Li (AL), and Fangqiong Ling (FL). DMC, KH, and AL extracted and compiled the data. In case of uncertainties, these were discussed and resolved by consensus. DMC and FL curated the database.

## 2.3 Data extraction

<https://automeris.io/WebPlotDigitizer>) was used to retrieve the information using digitized versions of figures. The qPCR/dPCR measurements themselves and the units (*i.e.*, quantitative cycles (Ct) or viral RNA levels) were recorded. In

addition, metadata about a sample was retrieved, including the study information, sample environment, and assay information. The study information included the author, title, and the year of publication. The sample environment included the following: i) the geographical location (*i.e.*, country and city where the study was performed), ii) the sampling location within a wastewater system (*i.e.*, samples were taken from the sewage collection systems, at the wastewater treatment plant after screenings and before sedimentation, or at the primary sedimentation tank), iii) sample processing prior to viral concentration (whether a sample was filtered, centrifuged, or left untreated), iv) the viral concentration method, v) the associated COVID case incidence or prevalence as provided in the publication, vi) the service population as provided in the publication, and vii) the date of collection of each wastewater sample. Finally, we extracted the assay information, including the choice of sampling techniques (*i.e.*, grab or composite sampling), qPCR/dPCR gene targets, and primer sets.

## 2.4 Data extraction and summary measures

Upon data retrieval, the SARS-CoV-2 measurements, sample environment, assay information, and COVID-19 case prevalence were recorded and converted to consistent units across studies (2.4.1–2.4.3). The proportion of positive detections was calculated (2.4.4). Annotated data are made available on <https://github.com/linglab-washu/wbe-metaanalysis> at the time of publication.

**2.4.1 SARS-CoV-2 measurements.** SARS-CoV-2 measurements in wastewater were retrieved in terms of copy numbers per mL, genome equivalents (ge) per mL, or copy numbers per gram, according to the way measurements were described in the Methods section of each study. A biosample is defined as a sewage specimen retrieved at a unique time and location. A biosample may be processed by multiple workflows, resulting in several SARS-CoV-2 measurements/observations per biosample. When the SARS-CoV-2 measurements of a biosample were performed in a simplex qPCR/dPCR using more than one genetic marker, each measurement per marker was entered as a unique observation. The sample size measured from a biosample is coded as  $n_{\text{biosample}}$  and the sample size measured by observations is coded as  $n_{\text{obs}}$ . To illustrate, if independent qPCR detections for N1, N2, and N3 were performed for a

**Table 1** Inclusion criteria for eligibility of studies

Inclusion criteria	Rationales
C1: qPCR data were reported as quantification cycles, copy numbers per volume, genome equivalents per mL, or genome equivalents per weight	C1 provides comparable data among studies
C2: sampling locations for raw sewage were identified as wastewater treatment plants (WWTPs), sewage collection networks, lift stations, manholes or septic tanks	C2 allows comparisons of SARS-CoV-2 viral titers and percent positivity in wastewater within and across studies
C3: COVID-19 case records were reported for the associated locations during the sampling times	C3 allows comparisons of SARS-CoV-2 viral titers in wastewater within and across studies



single biosample ( $n_{\text{biosample}} = 1$ ), each of the three marker measurements would be recorded as an independent observation, resulting in three observations ( $n_{\text{obs}} = 3$ ). Data entries (*i.e.*, observations) originating from the same biosample were annotated with the same sample ID if information linking observations and biosamples was made available in the publication. One study<sup>14</sup> reported the marker copies as ranges for a subset of data (*e.g.*, 1–10 N1 marker copies per mL). We recorded the midranges for these observations (*e.g.*, 5 N1 marker copies per mL). For studies reporting the average and standard deviations of multiple technical replicates for a wastewater sample, only the average was recorded. All eligible studies were included in the systematic review (3.1). Studies providing SARS-CoV-2 measurements as viral RNA levels or Ct were included in the analysis of positive detections (3.2, 3.4–3.7). Studies that provided viral RNA levels in terms of gene copies per unit volume were included in the analysis of SARS-CoV-2 viral RNA levels (3.3–3.7).

**2.4.2 Sample environment and assay information.** The sample environment and assay information were usually described in free texts and hence manual curation was performed. Some sample environment and assay information had a higher level of semantic consistency (*e.g.*, grab *vs.* composite samples), while others were described in more varied texts. In the case that varied descriptions had suggested similar meanings, we annotated using consistent texts reflecting the common meanings to facilitate synthesis across studies.

**Sampling location.** Specifically, the sampling locations were annotated as i) “WWTP” if the sample was described as taken after primary screenings and before the primary sedimentation tanks, as ii) “municipal sewage network” if the sample was taken from manholes, septic tanks, or lift stations, and as iii) “in premise” if the sample was described as taken from the private sewage infrastructure of a facility such as a hospital or a dormitory.

**Fractions.** Wastewater and sludge samples are included in the review. Wastewater refers to samples collected from the sewage network or the WWTP, consisting predominantly of a liquid phase and to a lesser degree, a solid phase. The term sludge specifically refers to the slurry of a solid and liquid mixture collected from a primary clarifier. The liquid and solid phases of samples can be separated/fractionated by laboratory methods. Fractions resulting from sample separation processes were recorded and annotated. Specifically, a fraction was annotated as “solids” when it consisted of primary solids from a gravity thickener, or solids collected from wastewater by in-laboratory sedimentation (*e.g.*, pellets recovered by centrifugation of the wastewater sample at >1000g). A fraction was annotated as “supernatant/filtrate” if the sample was pre-filtered at 0.22 to 0.7  $\mu\text{m}$  or centrifuged at 1000–10 000g before viral concentration. A fraction was annotated as “mixture of supernatant and suspended solids” when a sample of raw unprocessed wastewater was directly used for viral concentration.

**Viral concentration.** A fraction might be subjected to a subsequent viral concentration step. Typically, viral concentration methods were applied to a mixture of supernatant and suspended solids and supernatant/filtrate fractions. Solid fractions were not typically subjected to a viral concentration step. Viral concentration methods were recorded as described in the original publication.

**Gene targets.** Several SARS-CoV-2 qPCR gene targets were identified during the study screening process and categorized in the “marker” variable. Targeted regions included ORF1ab, nucleoprotein (N), spike protein (S), envelope protein (E), membrane protein (M), and the RNA-dependent RNA-polymerase (RdRp) gene. The specific primer set that was used to target the marker gene was recorded under the “primer” variable using the notation Author\_Marker. Two abbreviations were used in the field author, CDC, referring to the Center of Disease Control, USA (*e.g.*, CDC\_N1), and NIID, referring to the National Institute of Infectious Disease, Japan (*e.g.*, NIID\_N).

In the cases that SARS-CoV-2 measurements were performed using a multiplex qPCR/dPCR assay, the value for the variable “primer” for this specific observation was recorded by listing the primer sets employed, spaced by an underscore sign. To illustrate, if RNA levels were estimated using a duplex qPCR assay employing CDC\_N1 and CDC\_N2 primer sets, the value for the variable “primer” would be recorded as CDC\_N1\_N2. In some instances, a study may analyze multiple markers independently but report genome equivalents. A singular primer set would be recorded in the “primer” variable if it was specified in the study which primer set was used to calculate the reported genome equivalents; alternatively, the value recorded for the “primer” variable in the observation would include all the primer sets used in the study separated by a comma (*e.g.*, CDC\_N1, CDC\_N2).

**2.4.3 COVID-19 case prevalence.** Daily cases, cumulative cases, and active cases as reported in the publications were retrieved and included in this analysis, with exceptions when i) a sample was collected before epidemiological reporting by local health authorities was available or ii) a sample was collected from sewage lines in buildings in which the incidence of SARS-CoV-2 may significantly differ from city/municipality case reports. Sample entries for which consistent case prevalence data were not found in the study were excluded from the analysis. Case data were recorded in the way that was reported in the study. One study (*i.e.*, Gonzalez, R. *et al.*) reported data from WWTPs that extend over multiple municipalities.<sup>9</sup> For this study, the case incidence was estimated by computing the average of the case incidence (normalized by population size) of the municipalities contributing to the sewage of that specific WWTP.

$$C_{\text{WWTP}} \approx \frac{\sum_{i=1}^n \frac{C_i}{P_i}}{n}$$

where  $C_{\text{WWTP}}$  denotes the approximate cases for the WWTP,  $C_i$  is the case records for municipality,  $P_i$  is the population reported



for municipality<sub>*i*</sub>, and *n* is the total number of municipalities contributing wastewater to the WWTP.

Epidemiological data reported as “cumulative cases” are denoted as “cumulative cases”. Cases reported as “daily new cases”, “new cases”, “positive daily test”, “new positive daily test”, or “seven-day average cases” were denoted as “daily cases”. “Hospital admissions” and “hospitalized patients” were denoted as “hospitalized cases”. All case counts were converted to prevalence, *i.e.*, patients per 100 000 inhabitants, to allow synthesis across studies.

**2.4.4 Proportions of positive detection.** Subgroups were defined by different aggregating variables such as the study ID, sample collection method, and fraction type. The proportion of positive detection was defined as the ratio of observations showing positive test results for SARS-CoV-2 in a subgroup, over the total number of observations included in each subgroup.

## 2.5 Forest plot generation

Forest plots were generated using the “dmetar” package in *R* (ref. 28) employing a random-effects model. A random-effects meta-analysis model assumes that the observed average SARS-CoV-2 viral RNA levels can vary across studies because of real differences in the viral abundance in each system, as well as sampling variability (chance). Thus, even if all studies had an infinitely large sample size, the observed study effects would still vary because of the real differences in the sewershed’s effects on viral RNA levels. Such heterogeneity in average viral RNA levels can be caused by differences in study populations (such as local COVID-19 case prevalence), the wastewater system effects on dilution or decay, the methodological differences, and other factors.<sup>29–31</sup>

The weight of each study in the forest plot was calculated as

$$W_i = 1/(V_i + T^2)$$

where  $W_i$  denotes the weight of study<sub>*i*</sub>,  $V_i$  is the variance of study<sub>*i*</sub>, and  $T^2$  (tau) is the variance of each distribution concerning the grand mean estimated using the Sidik-Jonkman estimator.<sup>32</sup> More details on the calculations can be found in Borenstein *et al.*<sup>33</sup> Measurements of SARS-CoV-2 viral RNA levels were transformed into log gene copies per mL of sample to allow synthesis across studies and aid with visualization. Observations with SARS-CoV-2 measurements equal to zero marker copies per mL were removed before logarithmic transformation (observations removed = 815). Cubic root transformation of SARS-CoV-2 marker copies per mL was also performed to preserve true zero values. Forest plots were generated using both types of transformed data.

## 2.6 General linear mixed-effects model (GLMM)

General linear mixed-effects models were built to examine the epidemiological indicators (cumulative cases or daily new cases) as sources of fixed effects and studies as sources of random effects on SARS-CoV-2 measurements in wastewater.

A binomial GLMM was used to model the positive detections among all observations. A linear mixed-effects model (Gaussian) was used to fit the log-transformed viral RNA levels using observations in which positive detections were made. GLMMs were built in the *R* package “lme4”.<sup>34</sup> Studies were treated as sources of random effects on intercepts. Fixed-effects models were built using the same link functions to examine the significance of random effects and assess the overall fits from fixed effects. Fitting of fixed-effects models was performed using the “glm” and “lm” functions in the *R* stats package.<sup>35</sup> The Akaike information criterion (AIC), Bayesian information criterion (BIC), and log-likelihoods were reported for model selection. Nakagawa’s *R*-squared definitions were used to compute marginal and conditional *R*-squared values using the *R* package “MuMIn”.<sup>36</sup> The studies that reported daily cases and cumulative cases were examined separately. Studies reporting solids were excluded due to a lack of replicates after being subset into studies reporting daily cases or cumulative cases (details can be found in Fig. S1†).

### 3. Results

### 3.1 Systematic review

Our search identified 101 unique titles and abstracts; after screening (Fig. 1, Table S2†), 20 papers were included in this review. These studies reported SARS-CoV-2 measurements in wastewater in terms of viral RNA levels or Ct and provided epidemiological indicators. A total of 1751 observations were recorded. Fig. 1 depicts the details of the search.

Table 2 describes the basic characteristics of the included resources. Eighteen studies reported quantitative measurements for SARS-CoV-2 as gene copies per unit mass/volume,<sup>8,9,11,14–21,23,30,37–41</sup> while two studies reported Ct values.<sup>10,13</sup> Among the 18 quantitative studies, seventeen reported marker copies or genome equivalents per mL,<sup>8,9,14–21,23,30,37–41</sup> and one study reported marker copies per gram of biomass.<sup>11</sup> Epidemiological indicators were reported as daily cases in nine studies, ranging from 0.6 per 100 000 inhabitants to 117 per 100 000 inhabitants,<sup>11,13,14,16,18,19,21,39,41</sup> cumulative cases were reported in ten studies ranging from 1.6 per 100 000 inhabitants to 808 per 100 000 inhabitants,<sup>8,9,14,15,18,20,30,37,40,41</sup> active cases were reported in four studies<sup>10,21,38,40</sup> and hospitalized cases in two studies.<sup>13,17</sup> Among these studies, two studies reported both daily and cumulative cases,<sup>18,41</sup> one study reported both daily and active cases,<sup>21</sup> and one reported both cumulative cases and hospitalized cases.<sup>13</sup> Cumulative COVID-19 cases were the most frequently reported, followed by daily, active, and hospitalized cases. SARS-CoV-2 was detected in all studies, irrespective of case prevalence levels, albeit at varying proportions of positive detections.

Correlations between COVID-19 cases and wastewater SARS-CoV-2 viral RNA levels were reported in six studies. This is confirmed by our analysis. We performed linear regression on each dataset. Six out of eighteen studies detected

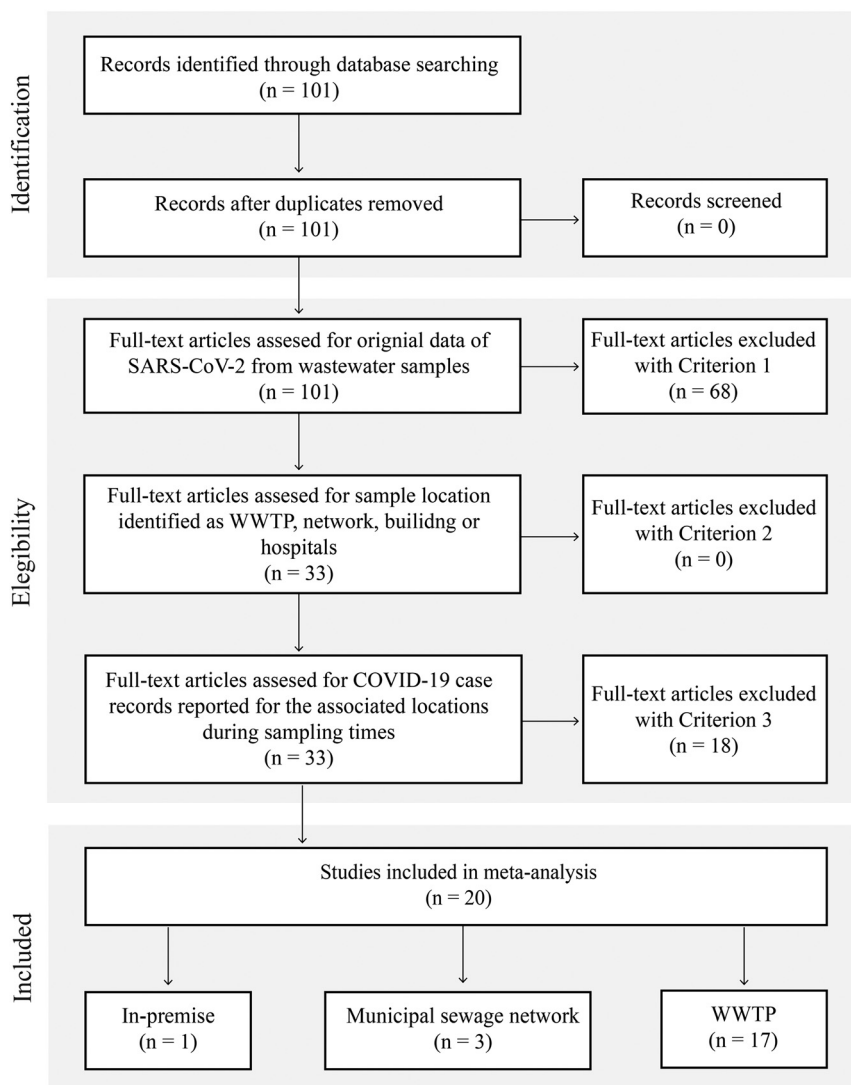


**Fig. 1** Study selection flow diagram. The three criteria used in the screening for eligibility are: criterion 1, original data of SARS-CoV-2 from wastewater samples were provided in terms of the quantification cycle (Ct), copy numbers per unit volume or weight, or genome equivalents per unit volume or weight; criterion 2, sampling locations were reported as WWTPs, sewage collection networks, buildings, or hospitals; criterion 3, COVID-19 case counts of the corresponding times and areas were reported in the study with a clear data source. Reports were found to be primarily sampling at WWTPs (17 studies) and less often at municipal sewage networks (3 studies) and in-premise (1 study); in-premise sampling was performed at a hospital.

significant linear correlations between SARS-CoV-2 viral RNA levels and the respective epidemiological indicators in the study ( $p$ -value < 0.05, Table 3, Fig. S2–S4†). These six studies were conducted at WWTPs, amongst which three analyzed the solid fraction, and three analyzed the supernatant/filtrate fraction.

Methodological variability was present in all steps of sample collection and analysis procedures (Fig. 2). In terms of sampling locations within a wastewater system, most studies analyzed samples collected at the WWTP (16 studies)<sup>8,9,11,12,14,16–21,23,37,38,40,41</sup>. A much smaller number of studies sampled at locations in the sewage collection network (two studies)<sup>13,39</sup> or in-premise (one study).<sup>13</sup> Kitamura, K. *et al.* examined the SARS-CoV-2 virus in wastewater at both municipal sewage network locations and WWTP influent

samples.<sup>15</sup> Saguti, F. *et al.* monitored WWTP influent samples and upstream locations.<sup>17</sup> Because case counts for biosamples collected at the sewage network in Saguti, F. *et al.* were not provided in the publication,<sup>17</sup> these biosamples from the upstream location were not included in the meta-analysis. Among the studies sampling at WWTPs, the service population ranged from 12 770 to 3.2 million individuals, and covered regions in the Americas ( $n_{\text{studies}} = 7$ ), Asia ( $n_{\text{studies}} = 4$ ), Europe ( $n_{\text{studies}} = 8$ ), and Oceania ( $n_{\text{studies}} = 1$ ).

Upon sample collection, studies showed great variability under sample pre-processing conditions, resulting in the enrichment of different wastewater fractions (Fig. 2). Supernatant/filtrate fractions were recovered in 12 studies using centrifugation between 1840 and 10 000g,<sup>8,9,11,14–19,30,37,40</sup> while two studies retrieved these fractions by filtrating raw wastewater



**Table 2** General features of studies included. COVID-19 cases are reported per 100 000 inhabitants unless otherwise stated. COVID-19 cases are rounded to the nearest unit.  $n_{\text{biosample}}$  indicates the number of unique sewage specimens analyzed,  $n_{\text{obs}}$  indicates the number of total measurements that were made for the SARS-CoV-2 virus

Author (biosamples, observations)	Country/date of sampling	Sample collection point	Sample type	Population served	Sample fraction	Viral concentration method	Type of case (mean, min, max)
Ahmed, W. <i>et al.</i> (2020) <sup>12</sup> ( $n_{\text{biosample}} = 8$ , $n_{\text{obs}} = 32$ )	Australia	Pumping station, WWTP influent	Grab and composite	736 172	Supernatant and suspended solids	Electronegative membrane absorption-direct RNA extraction	Cumulative cases (50, 0, 70)
Baldovin, T. <i>et al.</i> (2021) <sup>13a</sup> ( $n_{\text{biosample}} = 9$ , $n_{\text{obs}} = 18$ )	Feb–April, 2020 Italy	Municipal sewage network	Grab	12 770–36 042	Supernatant	Ultrafiltration (Centricon)	Cumulative cases (169, 141, 205)
D'Aoust, P. M. <i>et al.</i> (2021) <sup>21</sup> ( $n_{\text{biosample}} = 22$ , $n_{\text{obs}} = 44$ )	April 23 and May 05, 2020 Canada	Postgrid solids	Grab and composite	1 300 000	Solids	PEG precipitation	Hospitalized cases (34, 30, 39)
	April–June, 2020	Primary sludge				Alum precipitation–ultrafiltration	Daily cases (117, 19, 572)
Gonçalves, J. <i>et al.</i> (2021) <sup>10a</sup> ( $n_{\text{biosample}} = 15$ , $n_{\text{obs}} = 30$ )	June, 2020 Slovenia	Hospital sewage	Composite	N/A	Supernatant	Ultrafiltration	Active cases (19, 6, 58)
Gonzalez, R. <i>et al.</i> (2020) <sup>9</sup> ( $n_{\text{biosample}} = 198$ , $n_{\text{obs}} = 594$ )	March–May, 2020 USA	WWTP influent	Grab and composite	1 700 000	Supernatant	Hollow fiber concentrating pipet Adsorption–elution electronegative membrane	Cumulative cases <sup>b</sup> (2, 0, 4)
Graham, K. <i>et al.</i> (2020) <sup>11</sup> ( $n_{\text{biosample}} = 89$ , $n_{\text{obs}} = 166$ )	March–April, 2020 USA	WWTP influent	Composite	1 700 000	Supernatant	PEG precipitation	Active cases <sup>b</sup> (2, 0, 4)
	March–July, 2020	Primary settling tank	Composite		Primary solids	No concentration	Cumulative cases (229, 1, 2288)
Haramoto, E. <i>et al.</i> (2020) <sup>41</sup> ( $n_{\text{biosample}} = 5$ , $n_{\text{obs}} = 36$ )	March–May, 2020 Japan	WWTP influent	Grab	817 192 <sup>a</sup>	Supernatant and suspended solids	Electronegative membrane vortex–ultrafiltration	Daily cases (2, 1, 12)
						Electronegative membrane absorption-direct RNA extraction	Cumulative cases (5, 0, 7)
Hata, A. <i>et al.</i> (2021) <sup>14</sup> ( $n_{\text{biosample}} = 45$ , $n_{\text{obs}} = 87$ )	March–April, 2020 Japan	WWTP influent	Grab	697 000	Supernatant	PEG precipitation	Daily cases (1, 0, 1.0)
Kitamura, K. <i>et al.</i> (2021) <sup>15</sup> ( $n_{\text{biosample}} = 32$ , $n_{\text{obs}} = 198$ )	June–August, 2020 Japan	WWTP influent, municipal sewage network	Grab	N/A	Supernatant	Adsorption–elution electronegative membrane	Daily cases (8, 0, 19)
					Solids	PEG precipitation ultrafiltration	Cumulative cases (15, 0, 26)
Kumar, M. <i>et al.</i> (2020) <sup>37</sup> ( $n_{\text{biosample}} = 2$ , $n_{\text{obs}} = 6$ )	May, 2020 India	WWTP influent	Grab	N/A	Supernatant	Solid precipitation–centrifugation	Cumulative cases <sup>b</sup> (122, 19, 209)
Medema, G. <i>et al.</i> (2020) <sup>8</sup> ( $n_{\text{biosample}} = 25$ , $n_{\text{obs}} = 100$ )	Feb–March, 2020 Netherlands	WWTP influent	Composite	2 800 000	Supernatant	PEG precipitation	Cumulative cases <sup>b</sup> (7793, 4912, 10 674)
Miyani, B. <i>et al.</i> (2020) <sup>39</sup> ( $n_{\text{biosample}} = 33$ , $n_{\text{obs}} = 33$ )	April–May, 2020 USA	Municipal sewage network	Grab	3 200 000	Supernatant and suspended solids	Ultrafiltration (Centricon)	Cumulative cases (16, 0, 87)
Nemudryi, A. <i>et al.</i> (2020) <sup>16</sup> ( $n_{\text{biosample}} = 17$ , $n_{\text{obs}} = 34$ )	March–June, 2020 USA	WWTP influent	Composite	49 831	Supernatant	Adsorption–elution electropositive column filters	Daily cases (6, 4, 8)
						Ultrafiltration	Daily cases (6, 0, 14)



Author (biosamples, observations)	Country/date of sampling	Sample collection point	Sample type	Population served	Sample fraction	Concentration method	Type of case
Peccia, J. <i>et al.</i> (2020) <sup>23</sup> ( $n_{\text{biosample}} = 73$ , $n_{\text{obs}} = 226$ )	USA March–June, 2020	Primary settling tank	Grab	200 000	Solids	No concentration	Daily positive test (26, 3, 60)
Randazzo, W. <i>et al.</i> (2020) <sup>38</sup> (a) ( $n_{\text{biosample}} = 12$ , $n_{\text{obs}} = 24$ )	Spain Feb–April, 2020	WWTP influent	Grab	1 200 000	Supernatant and suspended solids	Aluminium flocculation	Active cases (80, 1, 111)
Randazzo, W. <i>et al.</i> (2020) <sup>20</sup> (b) ( $n_{\text{biosample}} = 42$ , $n_{\text{obs}} = 42$ )	Spain March–April, 2020	WWTP influent	Grab	1 357 177	Supernatant and suspended solids	Aluminum hydroxide adsorption–precipitation	Cumulative cases (36, 0, 140)
Saguti, F. <i>et al.</i> (2021) <sup>17</sup> ( $n_{\text{biosample}} = 21$ , $n_{\text{obs}} = 21$ )	Sweden February–July, 2020	WWTP influent	Composite	800 000	Supernatant	PS hollow fiber concentrating pipette Adsorption–elution electropositive cartridges–ultrafiltration	Newly hospitalized patients per day (9, 0, 20)
Sherchan, S. P. <i>et al.</i> (2020) <sup>18</sup> ( $n_{\text{biosample}} = 7$ , $n_{\text{obs}} = 28$ )	USA Jan–April, 2020	WWTP influent	Grab and composite	290 321	Supernatant and suspended solids	Adsorption–elution electronegative membrane	Cumulative cases (808, 0, 2534)
Trottier, J. <i>et al.</i> (2020) <sup>19</sup> ( $n_{\text{biosample}} = 7$ , $n_{\text{obs}} = 14$ )	France May–July, 2020	WWTP influent	Composite	470 000	Supernatant	Ultrafiltration	Daily cases (16, 0, 32) Daily cases (1, 0, 2)
Westhaus, S. <i>et al.</i> (2021) ( $n_{\text{biosample}} = 9$ , $n_{\text{obs}} = 18$ )	Germany April 08, 2020	WWTP influent	Composite	4 429 500	Supernatant	Ultrafiltration	Cumulative cases (123, 72, 220) Active cases (72, 30, 174)

<sup>a</sup> Semiquantitative studies. <sup>b</sup> Cases not normalized by 100 000 inhabitants.

through 0.22 (ref. 13) and 0.7  $\mu\text{m}$  membranes,<sup>10</sup> respectively. Mixed supernatant and suspended solid fractions were identified in six studies where liquid wastewater samples were not subjected to any type of pre-processing. Solid fractions were retrieved in one study from influent wastewater by pellet collection after centrifugation at 1840g,<sup>15</sup> while the remaining three studies utilizing solid fractions collected sludge samples directly from primary sedimentation tanks.<sup>11,21,23</sup> It is important to highlight that a study may pre-process for more than one fraction (Table 2).

Once a fraction of choice was generated, a viral concentration step was usually performed prior to RNA extraction. The viral concentration protocols relied on the principles of the molecular weight cutoff achieved through ultrafiltration at 10 000 Da,<sup>8,10,13,15,16,18,19,30,40</sup> the affinity of enveloped viruses to electro-negative membranes, electro-positive membranes, or other adsorbents/flocculants such as PEG, skimmed milk, or aluminum,<sup>9,11,14,15,18,20,21,30,37–39,41</sup> or a combination of both mechanisms sequentially.<sup>17,21,41</sup> Some protocols did not include a concentration step and performed RNA extraction directly on the solid fraction.<sup>17,23</sup> The methodological choices in the concentration step were highly variable, and the twelve different workflows were reported. Reviews on the viral concentration methodology and method evaluation employing surrogates can be found elsewhere.<sup>30,31,42–47</sup>

Notably, the various choices in separation methods result from an underlying assumption of differential enrichment/partitioning of the viral particles within the fractions in a biosample. Therefore, we considered the fractions as subgroups in achieving pooled estimates of SARS-CoV-2 RNA levels in wastewater (3.2).

### 3.2 Meta-analysis on the percentage of SARS-CoV-2 positive detections from untreated wastewater

While all the current studies took place during the COVID-19 pandemic, the detections of SARS-CoV-2 from wastewater were not always positive. We first ask, what was the grand mean of positivity of detection among studies taking place in the first year of wastewater-based SARS-CoV-2 monitoring? We examined the overall positivity across 1751 observations in 20 studies, which was 0.68 (95%-CI [0.52; 0.85]). Because the sampling mode (*i.e.*, grab or composite sampling) and fractions for analysis (*i.e.*, supernatants/filtrates, mixed supernatant and suspended solids, and solids only) were expected to introduce variations, we examined the means of the proportion of positive detection by sampling modes (Fig. 3) or fractions analyzed (Fig. 4). Wastewater SARS-CoV-2 measurements in composite sampling mode had a detection rate of 0.70 and a 95%-CI of [0.47; 0.94], whereas those generated from the grab sampling had an average detection



**Table 3** Regression coefficients for individual studies correlating SARS-CoV-2 measurements in wastewater (copies per mL) with COVID-19 case data of associated locations

Daily new COVID-19 cases per 100 000 inhabitants			
Author	Linear regression		
	Slope	R-Squared	p-Value
D'Aoust, P. M. <i>et al.</i>	0.52	0.51	$1.03 \times 10^{-7}$
Graham, K. <i>et al.</i>	196.64	0.35	$3.99 \times 10^{-17}$
Scherchan, S. P. <i>et al.</i>	0.03	0.17	$1.44 \times 10^{-1}$
Peccia, J. <i>et al.</i>	1994.77	0.16	$2.79 \times 10^{-10}$
Hata, A. <i>et al.</i>	0.16	0.05	$3.85 \times 10^{-2}$
Miyani, B. <i>et al.</i>	-0.20	0.01	$5.10 \times 10^{-1}$
Haramoto, E. <i>et al.</i>	-4.14	0.00	$7.29 \times 10^{-1}$
Trottier, J. <i>et al.</i>	0.19	0.00	$8.54 \times 10^{-1}$
Nemudryi, A. <i>et al.</i>	-0.02	0.00	$7.65 \times 10^{-1}$
Cumulative COVID-19 cases per 100 000 inhabitants			
Author	Linear regression		
	Slope	R-Squared	p-Value
Gonzalez, R. <i>et al.</i>	0.04	0.61	$4.81 \times 10^{-124}$
Medema, G. <i>et al.</i>	14.82	0.40	$1.30 \times 10^{-9}$
Scherchan, S. P. <i>et al.</i>	0.00	0.09	$2.87 \times 10^{-1}$
Haramoto, E. <i>et al.</i>	-4.62	0.08	$9.81 \times 10^{-2}$
Hata, A. <i>et al.</i>	0.08	0.03	$1.19 \times 10^{-1}$
Westhaus, S. <i>et al.</i>	-0.01	0.01	$6.63 \times 10^{-1}$
Randazzo, W. <i>et al.</i> (b)	0.45	0.01	$5.79 \times 10^{-1}$
Active COVID-19 cases per 100 000 inhabitants			
Author	Linear regression		
	Slope	R-Squared	p-Value
D'Aoust, P. M. <i>et al.</i>	3.85	0.33	$4.70 \times 10^{-5}$
Randazzo, W. <i>et al.</i> (a)	1.61	0.11	$1.19 \times 10^{-1}$
Westhaus, S. <i>et al.</i>	-0.01	0.01	$7.28 \times 10^{-1}$

rate of 0.57 and a 95%-CI of [0.34; 0.81]. The SARS-CoV-2 viral detection from the composite sampling approach was significantly higher than that from the grab sample mode (one-sided *t*-test,  $p_{\text{BH-adjusted}} = 5.63 \times 10^{-9}$ ). When grouped by the fraction analyzed, the supernatant, mixed supernatant and suspended solids, and solid fractions exhibited positive proportions of 0.53 (95%-CI [0.32; 0.75]), 0.62 (95%-CI [0.12; 1]), and 0.82 (95%-CI [0.43; 1]), respectively. Solids and solid-supernatant mixtures had a significantly higher average positive proportion than the supernatant/filtrate fraction ( $p_{\text{BH-adjusted}} < 2.00 \times 10^{-16}$  and  $p_{\text{BH-adjusted}} = 2.60 \times 10^{-10}$  in the pairwise *t*-test, respectively). Solid analysis exhibited a significantly higher average positive proportion than the solid-supernatant mixtures ( $p_{\text{BH-adjusted}} = 6.50 \times 10^{-8}$ ). It should be noted that even within subgroups, high heterogeneity ( $I^2$  0.97–0.99) was revealed from the meta-analysis. This could be caused by variations in COVID-19 cases or other local variables associated with a study, which will be explored in the regression analysis in section 3.4.

### 3.3 Meta-analysis of SARS-CoV-2 RNA levels in untreated wastewater

We focused on studies that reported SARS-CoV-2 RNA levels as gene copies per volume to calculate a pooled estimate of SARS-

CoV-2 RNA abundance in wastewater. These are seventeen studies including a total of 1508 out of 1674 quantitative observations. Across these studies, the average SARS-CoV-2 RNA abundance was 5244 gene copies per mL (95%-CI [0; 16 432]). We then aggregated studies by the fraction analyzed, *i.e.*, supernatants/filtrates, mixed supernatant and suspended solids, and solids. A forest plot showing the study means, weighted subgroup means, and confidence intervals is shown in Fig. 5. The average viral RNA levels in the wastewater supernatant, mixture, and solids are 50 gene copies per mL (95%-CI [0; 137],  $n_{\text{obs}} = 1009$ ), 181 gene copies per mL (95%-CI [0; 511],  $n_{\text{obs}} = 165$ ), and 30 456 gene copies per mL (95%-CI [0; 161 833],  $n_{\text{obs}} = 334$ ), respectively. The viral RNA levels from solid fractions exhibited significantly higher means than the other two groups ( $p_{\text{BH-adjusted}} < 2.00 \times 10^{-16}$  for both comparisons), yet the other two groups did not significantly differ ( $p_{\text{BH-adjusted}} > 0.97$ ). This finding suggests that once the viral RNA levels were beyond the detection limits, the difference between analyzed supernatants/filtrates and the mixture was not as strong.

Notably, viral RNA levels varied largely even among studies investigating SARS-CoV-2 RNA levels in the same sample fractions, as shown by heterogeneity across studies ( $I^2$  higher than 95% in all subgroups (Fig. 5, S5:† cubic root transformed data). We further aggregated the observations by grab/composite sampling and focused on studies that



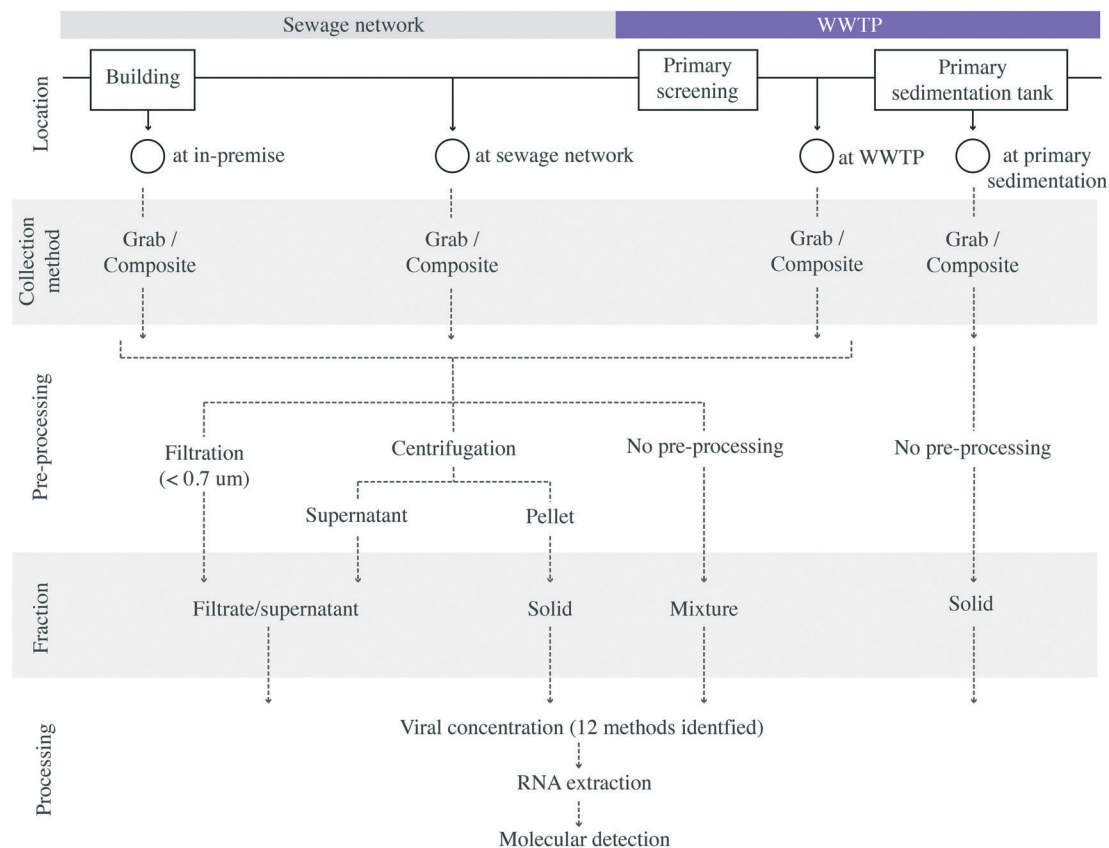


Fig. 2 Diagram depicting reported sample collection locations, pre-processing methodologies, and their respective annotations as sampling locations and fractions in this study.

reported WWTP observations alone (Fig. S6 and S7† cubic root transformed data). The cross-study heterogeneity remained high ( $I^2 > 93\%$ ) even after data were aggregated in more methodologically homogeneous groups. The observed heterogeneity suggested that pandemic severity, as well as other local variables, may drive the variations in SARS-CoV-2 RNA levels among studies.

### 3.4 Correlation between SARS-CoV-2 viral RNA levels in wastewater and reported COVID-19 cases

The overall correlation between daily cases and SARS-CoV-2 RNA levels is 0.28 (95%-CI, [0.01; 0.51], Table S3†). The Pearson Rho between the cumulative cases and SARS-CoV-2 RNA levels was 0.29 (95%-CI, [-0.15; 0.73], Table S3†). For both kinds of epidemiological indicators, wastewater-based SARS-CoV-2 viral RNA levels exhibited an overall positive correlation. In composite samples, the Pearson Rho between the viral RNA levels and epidemiological indicators was 0.41 (95%-CI, [-0.08; 0.74]) and 0.53 (95%-CI, [-0.21; 0.88]) for daily and cumulative cases, respectively (Fig. S8†). In grab samples, the Pearson Rho between the viral RNA levels and epidemiological indicators was 0.17 (95%-CI, [-0.12; 0.43]) and 0.20 (95%-CI, [-0.33; 0.63]) for daily and cumulative cases, respectively (Fig. S8†). While composite samples showed stronger correlations, heterogeneity values remained

high within subgroups of studies utilizing this sampling methodology ( $I^2 > 81\%$ , Fig. S8†).

### 3.5 Covariates explaining variations in SARS-CoV-2 viral RNA levels in wastewater

We ask, how much of the large heterogeneity in the average copy numbers of SARS-CoV-2 in wastewater can be explained by the sampling mode, fraction analyzed, and COVID-19 case prevalence, respectively? To answer this question, we built univariate models focusing on each covariate, respectively. Studies reporting cumulative cases ( $n_{\text{obs}} = 912$ ,  $n_{\text{studies}} = 8$ ) and daily cases ( $n_{\text{obs}} = 500$ ,  $n_{\text{studies}} = 8$ ) were examined separately to ensure consistent within-group case reporting units.

First, we built logistic regression models to explain the relationships between positive SARS-CoV-2 detection from sewage and each covariate considered. The models with the sampling mode and fraction analyzed as sole predictors explained 0.6% and 12.4% (Tjur's  $R$ -squared) of the total variability in SARS-CoV-2 positive detections, respectively (Table 4). The proportion of variances explained by daily and cumulative cases was 9.3% and 5.9%, respectively (Table 5).

Next, we built linear models to examine the relationships between logarithmic transformed viral RNA levels and each covariate. The variance in RNA levels explained by the



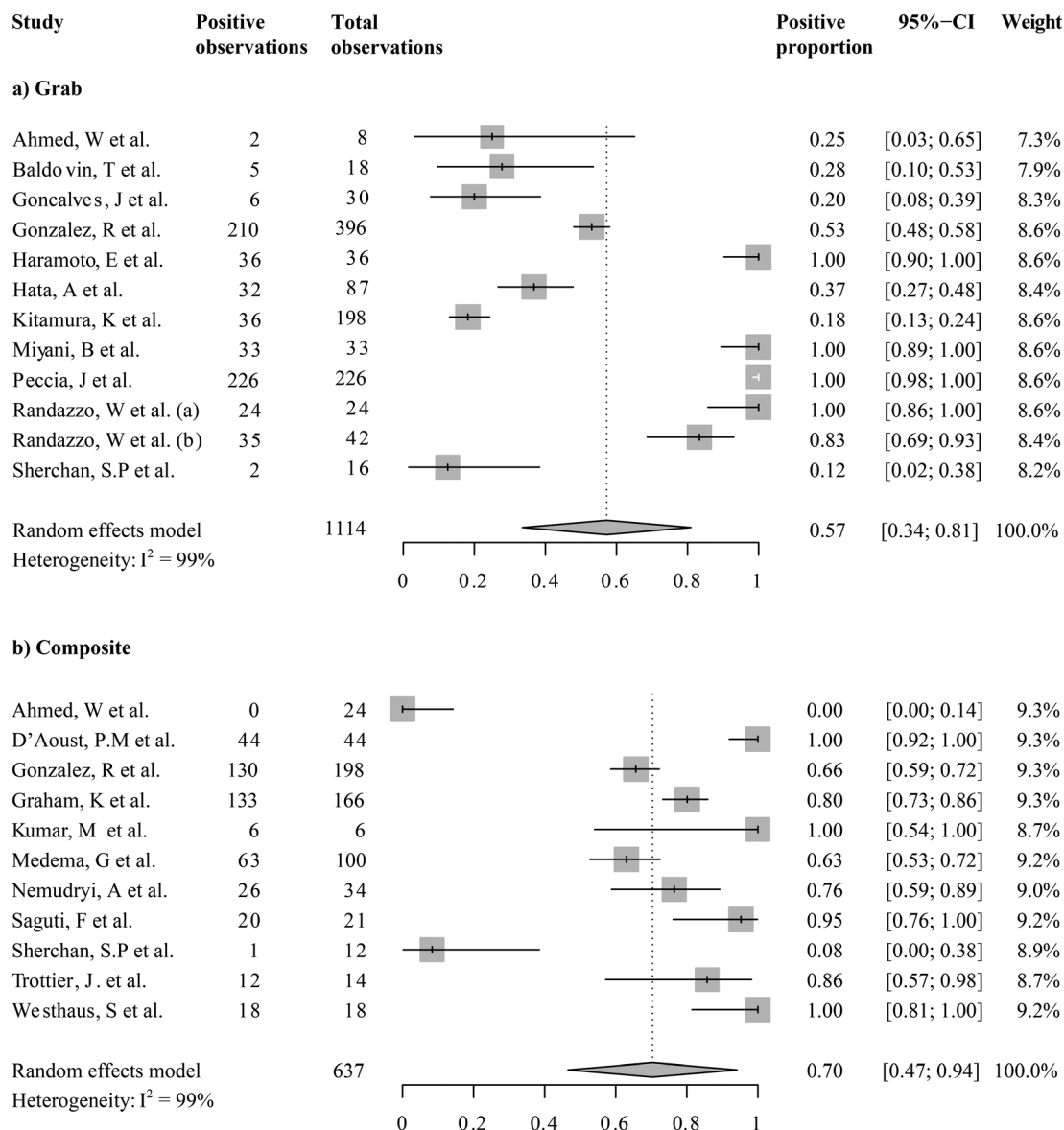


Fig. 3 Forest plot of selected aggregation reporting the proportions of positive detections for SARS-CoV-2 in wastewater samples. Pooled estimates for (a) all studies utilizing grab samples and (b) all studies utilizing composite samples.

sampling mode and fraction analyzed was 6.9% and a notable 56.0%, respectively, whereas the variance explained by daily and cumulative cases was 0.9% and 0.8%, respectively. In all these models, the roles of methodological variables and epidemiological indicators were significant ( $p < 0.05$ , Tables 4 and 5). The daily or cumulative cases and sampling mode explained comparable proportions of variances. Notably, the fraction analyzed explained dramatically higher variance in viral RNA levels than any other variables.

### 3.6 Slope coefficients in generalized linear models

Successful detection of the virus from wastewater is fundamental to WBE; our generalized linear models on positive detections can provide quantitative insights into the

magnitude at which changes in each variable increase the chance of the positive detections (Table 4 binomial family models and Table 5 binomial fixed-effects model). From our models, the odds of positive detection decrease by a factor of 1.43 (95%-CI [1.81; 1.13]) when utilizing grab sampling in contrast to composite sampling. The odds of positive detection increase by a factor of 8.16 (95%-CI [6.08; 12.92]) from solid fractions in contrast to supernatants/filtrates; they increase by a factor of 3.52 (95%-CI [2.43; 5.30]) from solid-supernatant mixtures in contrast to supernatants/filtrates. With an increase in active case prevalence of 10 per 100 000 inhabitants, the odds of positive detection increase by a factor of 1.06 units (95%-CI [1.04; 1.09]); with an increase in cumulative cases of 10 per 100 000 inhabitants, they increase by a factor of 1.02 (95%-CI [1.01; 1.03]).



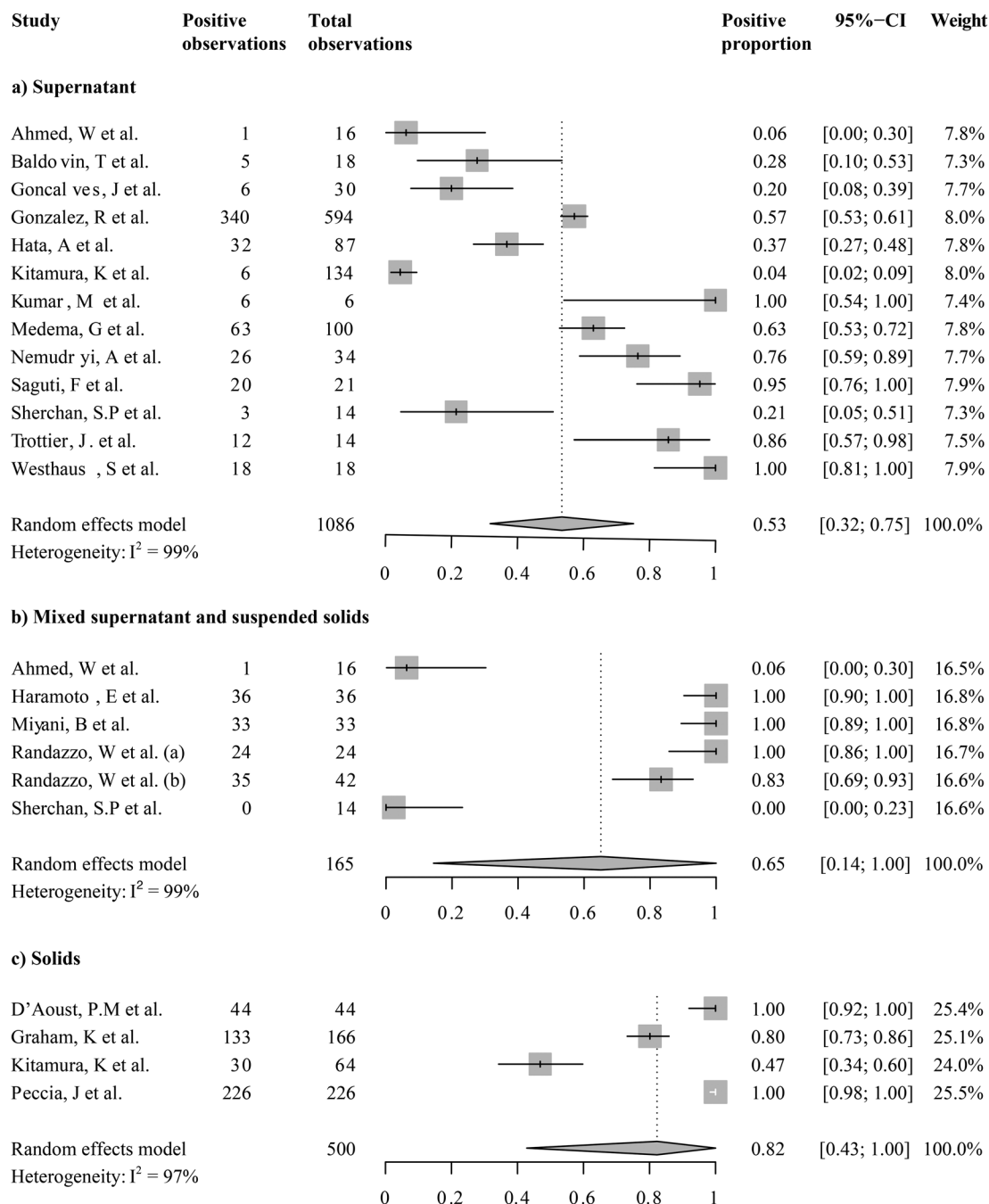


**Fig. 4** Forest plot of selected aggregation reporting the proportions of positive detections for SARS-CoV-2 in wastewater samples. Pooled estimates for (a) all studies analyzing supernatants/filtrates, (b) all studies analyzing mixtures without pre-processing, and (c) all studies analyzing solids.

### 3.7 Mixed-effects model helps account for variation by studies

While many applications of WBE rely on positive correlations between SARS-CoV-2 RNA levels in wastewater and disease prevalence, larger or comparable variability was explained by methodological covariates than the reported case prevalence in our models (Tables 4 and 5). While documenting methodological covariates in WBE studies is crucial, learning

about which variables are of importance in WBE studies is an ongoing process. To address the need of building explanatory or predictive models in WBE, we considered a mixed-effects framework for modeling SARS-CoV-2 viral RNA levels from multiple studies. Here, we treat studies as a collective source of variance. We hypothesize that in addition to the role of cases as a source of fixed effects on the wastewater measurements, each study presents a source of a study-specific intercept. We tested for the significance of random



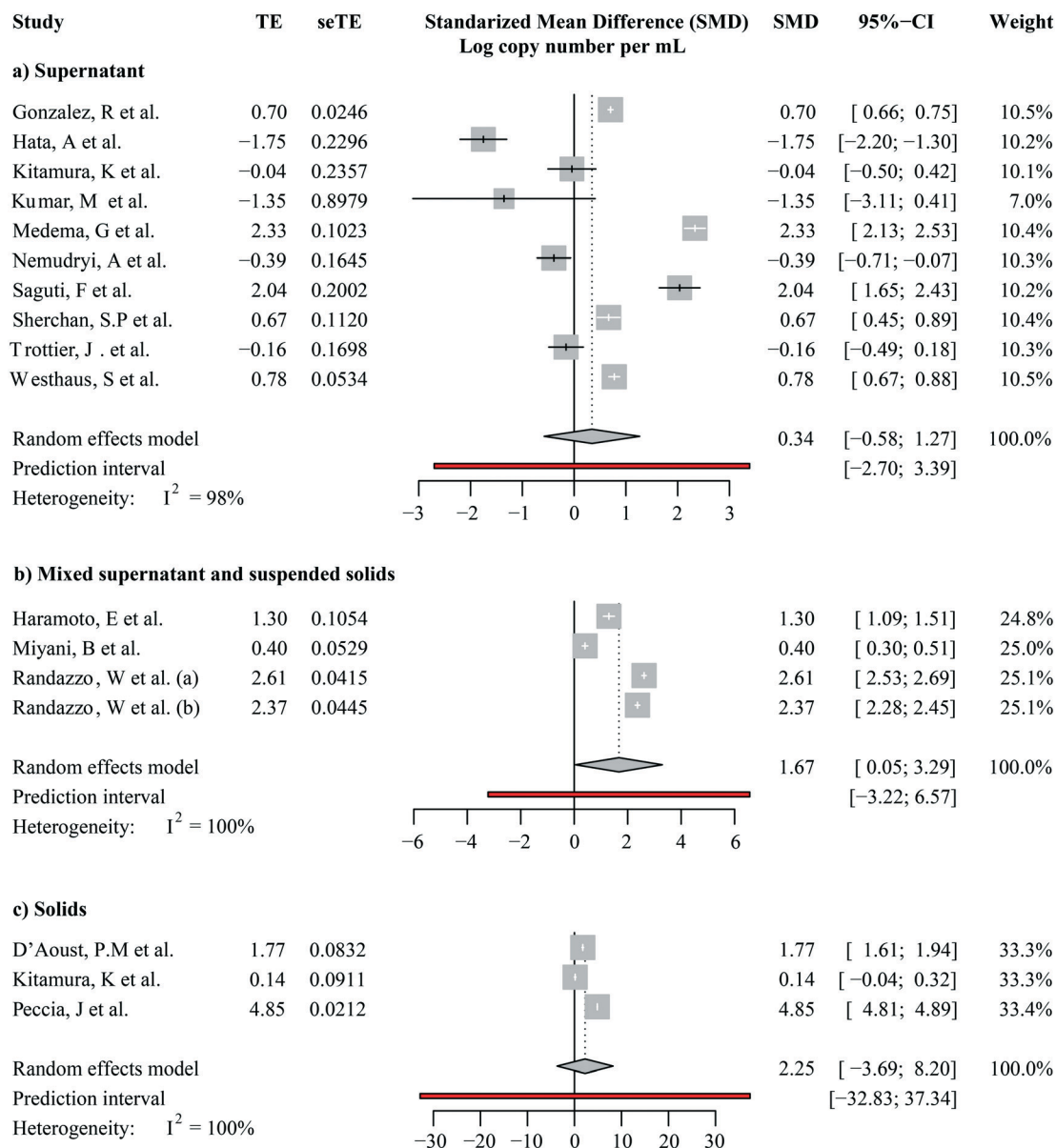


**Fig. 5** Forest plot of selected aggregation reporting weighted means of SARS-CoV-2 RNA levels in wastewater. Pooled estimates for (a) all studies analyzing supernatants/filtrates, (b) all studies analyzing mixtures without pre-processing, and (c) all studies analyzing solids. The forest plot includes data from all studies that reported SARS-CoV-2 RNA levels as gene copy numbers per unit volume. CI-confidence interval.

effects. For both, positivity or viral RNA levels from daily or cumulative cases, the random effects from the studies were significant ( $p$ -value  $< 2.00 \times 10^{-16}$ , Table 5). Mixed-effects models also showed a lower AIC or BIC than the corresponding fixed-effects models, suggesting better fits to the data.

For a mixed-effects model, we examined both the marginal  $R$ -squared, which is the proportion of variance explained by the fixed effects alone (daily or cumulative cases), and the conditional  $R$ -squared, which describes the proportion of variance explained by both the fixed and random factors (cases and the study identities respectively). Notably, mixed models exhibited conditional  $R$ -squared close to or over 0.9 for both positivity and viral RNA levels models reporting daily

new cases or cumulative cases (Table 5). Thus, simultaneously considering variability across studies greatly improved our ability to explain the variation in wastewater SARS-CoV-2 measurements.

## 4. Discussion

Sampling modes and wastewater fractions had strong influences on the pooled means in proportions of positive detection and SARS-CoV-2 RNA levels. The sampling mode explained 0.6% in the variance of positive detections. The composite sampling mode had a higher detection rate than grab sampling, as seen from an average detection rate of 0.70 (95%–CI, [0.47; 0.94]) and 0.56 (95%–CI, [0.32; 0.79], Fig. 3),



**Table 4** Methodological variables explaining variances in SARS-CoV-2 positive detections and RNA levels

Univariate models	Binomial ( $n_{\text{obs}} = 1508$ )			Gaussian (log transformation on RNA levels) ( $n_{\text{obs}} = 936$ )		
	Coefficient [95%-CI]	<i>p</i> -Values	Explained variance ( <i>R</i> -squared)	Coefficient [95%-CI]	<i>p</i> -Values	Explained variance ( <i>R</i> -squared)
Grab_composite			0.01			0.07
Intercept	0.75 [0.55, 0.95]	$2.1 \times 10^{-13***}$		2.50 [1.99, 2.98]	$<2.00 \times 10^{-16***}$	
Grab_composite: grab	-0.36 [-0.59, -0.12]	$2.84 \times 10^{-3**}$		2.54 [1.94, 3.14]	$3.10 \times 10^{-16***}$	
Fraction			0.12			0.56
Intercept	0.01 [-0.11, 0.13]	0.87		1.51 [1.25, 1.77]	$<2.00 \times 10^{-16***}$	
Fraction: solid	2.17 [1.8, 2.56]	$<2 \times 10^{-16***}$		7.53 [7.10, 7.96]	$<2.00 \times 10^{-16***}$	
Fraction: solid-supernatant mixture	1.27 [0.89, 1.67]	$1.9 \times 10^{-10***}$		2.14 [1.56, 2.72]	$9.70 \times 10^{-13***}$	

**Table 5** Fixed-effects and mixed-effects modeling of the effects of COVID-19 daily new cases or cumulative cases on the positive detection and titers of SARS-CoV-2 viruses in wastewater. CI: confidence interval, AIC: Akaike information criterion, BIC: Bayesian information criterion, Loglik: log likelihood

Model name	Daily case model ( $n_{\text{obs}} = 500$ , $n_{\text{studies}} = 8$ )				Cumulative case model ( $n_{\text{obs}} = 912$ , $n_{\text{studies}} = 8$ )			
	Binomial		Gaussian (log transformation on titers)		Binomial		Gaussian (log transformation on titers)	
	Fixed effects	Mixed effects	Fixed effects	Mixed effects	Fixed effects	Mixed effects	Fixed effects	Mixed effects
Fixed effects	<i>b</i> [95% CI]	<i>b</i> [95% CI]	<i>b</i> [95% CI]	<i>b</i> [95% CI]	<i>b</i> [95% CI]	<i>b</i> [95% CI]	<i>b</i> [95% CI]	<i>b</i> [95% CI]
Intercept	0.65 [0.33, 0.96]	3.32 [-1.35, 8.00]	6.23 [5.63, 6.84]	1.78 [-1.09, 4.66]	-0.03 [-0.20, 0.13]	-0.06 [-3.95, 3.83]	1.78 [1.53, 2.04]	1.05 [-1.25, 3.36]
Daily new cases	0.06 [0.04, 0.09]	0.11 [0.05, 0.16]	0.01 [0.001, 0.02]	0.01 [0.003, 0.009]	—	—	—	—
Cumulative cases	—	—	—	—	0.001 [0.001, 0.002]	0.005 [0.004, 0.007]	0.0007 [0.0001, 0.0013]	0.002 [0.001, 0.002]
Random effects								
Study_ID (variance)	—	23.15	—	17.12	—	29.75	—	10.93
Adjusted $R^2$	0.09	—	0.01	—	0.06	—	0.01	—
Marginal $R^2$	—	0.54	—	0.01	—	0.08	—	0.02
Conditional $R^2$	—	0.94	—	0.93	—	0.91	—	0.90
AIC	422	200	2579	1406	1214	1012	2381	1692
BIC	431	213	2591	1422	1224	1027	2394	1709
Loglik	-209	-97	-1287	-699	-605	-503	-1188	-842
Random effects ( <i>p</i> -values)	—	$<2.2 \times 10^{-16***}$	—	$<2.2 \times 10^{-16***}$	—	$<2.2 \times 10^{-16***}$	—	$<2.2 \times 10^{-16***}$

respectively. This observation is in agreement with the previous literature that showed improved SARS-CoV-2 detection in composite wastewater samples.<sup>48</sup> George, A. *et al.* (2022) showed that in liquid fractions composite sampling outperformed grab sampling on smaller geographical scales, such as neighborhood, city block, and building scales. While none of the primary research studies included passive sampling, this sampling strategy is in development<sup>49</sup> and worthy of consideration for future meta-analyses.

Supernatant/filtrate, solid-supernatant mixture, and solid fractions increased by average detection rates of 0.53 (95%-CI [0.32; 0.75]), 0.62 (95%-CI [0.12; 1]), and 0.82 (95%-CI [0.43; 1]), respectively (Fig. 4). The fraction analyzed explained 12.4% of the variance in the proportions of positive detection and 56% of the variance in RNA levels. Solid fractions exhibited SARS-CoV-2 viral RNA levels that were orders of

magnitude higher than supernatants/filtrates and solid-supernatant mixtures. This observation is in agreement with the previous literature showing enrichment of the SARS-CoV-2 genetic material in wastewater solids (*i.e.*, primary settled solids).<sup>50</sup> Given the higher proportion of SARS-CoV-2 viral RNA in solid fractions, workflows utilizing wastewater solids may be useful to track SARS-CoV-2 when infections remain at low levels in the sewershed (*i.e.*, periods between peaks of infection, early warning detection, *etc.*). The large variance in viral RNA levels explained by the fraction analyzed and the large magnitudes in regression coefficients suggest that standardizing the fraction analyzed needs to be prioritized when researchers would like to design monitoring efforts across multiple labs.<sup>47</sup> The overall detection rate and those in subgroups of any sewage fraction were below one, suggesting a need for tools to maximize the chance of SARS-CoV-2 detection from sewage samples.



In our meta-analysis, large heterogeneity was detected in all effect sizes investigated (*i.e.*, proportions of positive detections, viral RNA levels, and Pearson Rho between RNA levels and daily or cumulative cases, Fig. 3–5, Table S3†). We hypothesize that the unexplained variations in SARS-CoV-2 RNA levels detected in wastewater can be affected by study-level factors, such as COVID-19 prevalence, lags in epidemiological data reporting,<sup>51</sup> methodological choices,<sup>46</sup> and differences in the wastewater collection system design. Our meta-analysis found that metadata about the collection system, such as *per capita* water consumption, relative contributions of domestic *vs.* commercial/industrial water, or sewage travel times (*i.e.*, residence times), are currently rare. These collection system-level variables can affect the dilution of fecal materials and the genetic decay of the viral signal.<sup>31,52–54</sup> To illustrate, domestic water consumption can vary significantly in different areas, a person in the city of Berlin generates on average 135 L of wastewater per day,<sup>55</sup> while a person in Qatar generates on average 500 L of wastewater per day.<sup>56</sup> Thus, the dilution of the fecal matter may vary largely in different wastewater systems. Another aspect is combined sewage in comparison to sanitary sewage. Rainfall can affect the dilution of fecal matter in a combined sewage system through stormwater run-off,<sup>57,58</sup> while not so in a sanitary sewage system. Even among sanitary sewage, the contribution of domestic waste can vary by system, ranging from as low as 30% of the total wastewater discharge to as high as near-complete dominance.<sup>59</sup> These design differences could lead to variations in SARS-CoV-2 RNA levels even in systems where active viral shedders were identical.

Because water usage and system design characteristics can affect SARS-CoV-2 virus measurements at the wastewater treatment plant, more detailed metadata reporting regarding the wastewater collection system is needed to better explain variations across sites. McClary-Gutierrez, J. S. *et al.* compiled a list of minimum reporting data for WBE applications for COVID-19,<sup>60</sup> which can support more consistent metadata reporting across studies and facilitate the synthesis of results. Lately, it was proposed that wastewater can be viewed as an independent indicator of true prevalence, as epidemiological indicators from current reporting can be affected by under-reporting.<sup>61</sup> Therefore, methods and tools to investigate the wastewater metagenome and derive system-level data, or bridge wastewater-based measurements to prevalence, deserve more attention.<sup>62</sup>

To address the dilution of fecal matter by various wastewater streams, normalization of SARS-CoV-2 viral RNA levels by fecal strength indicators has been performed in some studies. These propose dividing the SARS-CoV-2 viral RNA levels by the copy numbers of pepper mild mottle virus (PMMoV),<sup>21,58,63</sup> a diet-associated RNA virus commonly found in human feces.<sup>64</sup> Among the qualified studies included in this meta-analysis, only one study utilized normalization by PMMoV,<sup>21</sup> thus a meta-analysis on the effect of PMMoV normalization on correlations between wastewater SARS-CoV-2 measurements and epidemiological indicators was not

included in this study. The effects of normalization techniques on the performance of regression models can be a topic of future interest in meta-analysis efforts when studies employing such techniques become more abundant.

It should be noted that heterogeneity in viral RNA levels and correlations observed here may not be fully explained by recovery efficiencies of viruses from wastewater samples during viral concentration workflows. To illustrate this complexity, we discuss two studies where recovery efficiencies were reported. In one study, an average viral RNA level of  $881 \pm 633$  marker copies per mL was detected when COVID-19 prevalence in the associated area was between 10 and 80 cumulative cases per 100 000 inhabitants;<sup>8</sup> in another study, an average viral RNA level of  $1.9 \pm 6.0$  marker copies per mL was reported within the same range of COVID-19 prevalence (10–80 cumulative cases per 100 000 inhabitants).<sup>9</sup> After adjusting the viral RNA levels by reported recovery efficiencies (73 and 7.7%, respectively), the adjusted copy numbers (1206 and 27 marker copies per mL, respectively) still vary by two orders of magnitude.

While the field's ability to quantify the effects of methodological variables and collection systems is an important ongoing research topic,<sup>46,47,65</sup> mixed-effects models treating “studies” as a source of random effects can be considered useful for performing inference and prediction. Mixed-effects models handle a wide range of scenarios where observations have been sampled in a hierarchical structure rather than completely independently. In this study, treating studies as a source of random effects on intercepts profoundly improved the quality of the model, as seen in improved AIC and BIC compared to the respective fixed-effects models (Table 5). The final models reached conditional *R*-squared values above 0.9. The mixed-effects approach provides an alternative for researchers to leverage existing data from studies conducted elsewhere to build models useful for explaining variations in local observations.

## 5. Study strengths and limitations

In summary, we synthesized the available evidence on SARS-CoV-2 detection and viral RNA levels in wastewater reported during the first year of the COVID-19 pandemic. The combined detection rate across studies was 67% (95%-CI, [0.56; 0.79]). Despite the large heterogeneity in SARS-CoV-2 RNA levels among methodologically similar studies (*i.e.*,  $93\% < I^2 < 100\%$ ), SARS-CoV-2 abundance in wastewater exhibited strong correlations with epidemiological indicators. These results reinforce that wastewater is a favorable data source to track COVID-19 dynamics in a community.

Our study had several limitations. The most notable is the large amount of unexplained heterogeneity in positive detection, SARS-CoV-2 RNA levels, and Pearson correlations across studies. This is likely attributable to variability in methodological differences in SARS-CoV-2 virus measurements, wastewater-system characteristics, ways the epidemiological data were collected and reported as well as



different COVID-19 incidence at the time the studies were conducted (e.g., COVID-19 waves and case fluctuations). Thus, we employed mixed-effects models to make inferences about the correlation between epidemiological indicators and viral detection/RNA levels, treating study-level variations as a source of random effects.

This systematic review and meta-analysis were performed using the Web of Science core collection focusing on the English-language literature. Other indexes such as PubMed, Medline, and Scopus are worth examining in future research. Sources such as Europe PMC which included preprint servers will increase data inclusion. As more data become available, future meta-analysis focusing on the collection of upstream sewage streams and comparisons of SARS-CoV-2 detection sensitivity between qPCR and dPCR may become possible. The present study may be used as a framework for future studies analyzing larger datasets.

## Conflicts of interest

There are no conflicts to declare.

## Acknowledgements

This work is supported by the N.S.F. CAREER Award 2047470 (F. L.) and Washington University Faculty Start-up Fund (F. L.).

## References

- 1 D. A. Larsen and K. R. Wigginton, *Nat. Biotechnol.*, 2020, **38**, 1151–1153.
- 2 Y. Chen, L. Chen, Q. Deng, G. Zhang, K. Wu, L. Ni, Y. Yang, B. Liu, W. Wang and C. Wei, *J. Med. Virol.*, 2020, **92**, 833–840.
- 3 F. Xiao, J. Sun, Y. Xu, F. Li, X. Huang, H. Li, J. Zhao, J. Huang and J. Zhao, *Emerging Infect. Dis.*, 2020, **26**, 1920.
- 4 M. Guo, W. Tao, R. A. Flavell and S. Zhu, *Nat. Rev. Gastroenterol. Hepatol.*, 2021, **18**, 269–283.
- 5 M. J. Binnicker, *J. Clin. Microbiol.*, 2020, **58**, e01695-20.
- 6 M. Murakami, A. Hata, R. Honda and T. Watanabe, *Environ. Sci. Technol.*, 2020, **54**, 5311–5311.
- 7 T. Hovi, L. M. Shulman, H. Van Der Avoort, J. Deshpande, M. Roivainen and E. M. De Gourville, *Epidemiol. Infect.*, 2012, **140**, 1–13.
- 8 G. Medema, L. Heijnen, G. Elsinga, R. Italiaander and A. Brouwer, *Environ. Sci. Technol. Lett.*, 2020, **7**, 511–516.
- 9 R. Gonzalez, K. Curtis, A. Bivins, K. Bibby, M. H. Weir, K. Yetka, H. Thompson, D. Keeling, J. Mitchell and D. Gonzalez, *Water Res.*, 2020, **186**, 116296.
- 10 J. Gonçalves, T. Koritnik, V. Mioč, M. Trkov, M. Bolješić, N. Berginc, K. Prosenc, T. Kotar and M. Paragi, *Sci. Total Environ.*, 2021, **755**, 143226.
- 11 K. E. Graham, S. K. Loeb, M. K. Wolfe, D. Catoe, N. Sinnott-Armstrong, S. Kim, K. M. Yamahara, L. M. Sassoubre, L. M. Mendoza Grijalva and L. Roldan-Hernandez, *Environ. Sci. Technol.*, 2021, (55), 488–489.
- 12 W. Ahmed, N. Angel, J. Edson, K. Bibby, A. Bivins, J. W. O'Brien, P. M. Choi, M. Kitajima, S. L. Simpson and J. Li, *Sci. Total Environ.*, 2020, **728**, 138764.
- 13 T. Baldovin, I. Amoroso, M. Fonzo, A. Buja, V. Baldo, S. Cocchio and C. Bertoncello, *Sci. Total Environ.*, 2021, **760**, 143329.
- 14 A. Hata, H. Hara-Yamamura, Y. Meuchi, S. Imai and R. Honda, *Sci. Total Environ.*, 2021, **758**, 143578.
- 15 K. Kitamura, K. Sadamasu, M. Muramatsu and H. Yoshida, *Sci. Total Environ.*, 2021, **763**, 144587.
- 16 A. Nemudryi, A. Nemudraia, T. Wiegand, K. Surya, M. Buyukyoruk, C. Cicha, K. K. Vanderwood, R. Wilkinson and B. Wiedenheft, *Cell Rep. Med.*, 2020, **1**, 100098.
- 17 F. Saguti, E. Magnil, L. Enache, M. P. Churqui, A. Johansson, D. Lumley, F. Davidsson, L. Dotevall, A. Mattsson and E. Trybala, *Water Res.*, 2021, **189**, 116620.
- 18 S. P. Sherchan, S. Shahin, L. M. Ward, S. Tandukar, T. G. Aw, B. Schmitz, W. Ahmed and M. Kitajima, *Sci. Total Environ.*, 2020, **743**, 140621.
- 19 J. Trottier, R. Darques, N. A. Mouheb, E. Partiot, W. Bakhache, M. S. Deffieu and R. Gaudin, *One Health*, 2020, **10**, 100157.
- 20 W. Randazzo, P. Truchado, E. Cuevas-Ferrando, P. Simón, A. Allende and G. Sánchez, *Water Res.*, 2020, **181**, 115942.
- 21 P. M. D'Aoust, E. Mercier, D. Montpetit, J.-J. Jia, I. Alexandrov, N. Neault, A. T. Baig, J. Mayne, X. Zhang and T. Alain, *Water Res.*, 2021, **188**, 116560.
- 22 P. M. D'Aoust, T. E. Graber, E. Mercier, D. Montpetit, I. Alexandrov, N. Neault, A. T. Baig, J. Mayne, X. Zhang and T. Alain, *Sci. Total Environ.*, 2021, **770**, 145319.
- 23 J. Peccia, A. Zulli, D. E. Brackney, N. D. Grubaugh, E. H. Kaplan, A. Casanovas-Massana, A. I. Ko, A. A. Malik, D. Wang and M. Wang, *Nat. Biotechnol.*, 2020, **38**, 1164–1167.
- 24 J. Gurevitch, J. Koricheva, S. Nakagawa and G. Stewart, *Nature*, 2018, **555**, 175–182.
- 25 M. H. Murad and V. M. Montori, *Jama*, 2013, **309**, 2217–2218.
- 26 A. H. Linden and J. Hönekopp, *Perspect. Psychol. Sci.*, 2021, **16**, 358–376.
- 27 M. J. Page, J. E. McKenzie, P. M. Bossuyt, I. Boutron, T. C. Hoffmann, C. D. Mulrow, L. Shamseer, J. M. Tetzlaff, E. A. Akl and S. E. Brennan, *BMJ*, 2021, (372), n71.
- 28 M. Harrer, P. Cuijpers, T. A. Furukawa and D. D. Ebert, *Doing Meta-Analysis with R: A Hands-On Guide*, Chapman and Hall/CRC, 2021.
- 29 X. Bertels, P. Demeyer, S. Van den Bogaert, T. Boogaerts, A. L. van Nuijs, P. Delpitte and L. Lahousse, *Sci. Total Environ.*, 2022, 153290.
- 30 W. Ahmed, P. M. Bertsch, A. Bivins, K. Bibby, K. Farkas, A. Gathercole, E. Haramoto, P. Gyawali, A. Korajkic, B. R. McMinn, J. F. Mueller, S. L. Simpson, W. J. M. Smith, E. M. Symonds, K. V. Thomas, R. Verhagen and M. Kitajima, *Sci. Total Environ.*, 2020, **739**, 139960.
- 31 A. I. Silverman and A. B. Boehm, *Environ. Sci. Technol. Lett.*, 2020, **7**, 544–553.
- 32 K. Sidik and J. N. Jonkman, *J. R. Stat. Soc., C: Appl. Stat.*, 2005, **54**, 367–384.



- 33 M. Borenstein, L. V. Hedges, J. P. Higgins and H. R. Rothstein, *Res. Synth. Methods*, 2010, **1**, 97–111.
- 34 D. Bates, M. Mächler, B. Bolker and S. Walker, ArXiv Prepr. ArXiv14065823, 2014.
- 35 R Core Team, Vienna R Core Team.
- 36 K. Barton, Http://Forge R-Proj. Org/projects/mumin.
- 37 M. Kumar, A. K. Patel, A. V. Shah, J. Raval, N. Rajpara, M. Joshi and C. G. Joshi, *Sci. Total Environ.*, 2020, **746**, 141326.
- 38 W. Randazzo, E. Cuevas-Ferrando, R. Sanjuán, P. Domingo-Calap and G. Sánchez, *Int. J. Hyg. Environ. Health*, 2020, **230**, 113621.
- 39 B. Miyani, X. Fonoll, J. Norton, A. Mehrotra and I. Xagorarakis, *J. Environ. Eng.*, 2020, **146**, 06020004.
- 40 S. Westhaus, F.-A. Weber, S. Schiwy, V. Linnemann, M. Brinkmann, M. Wiedera, C. Greve, A. Janke, H. Hollert and T. Wintgens, *Sci. Total Environ.*, 2021, **751**, 141750.
- 41 E. Haramoto, B. Malla, O. Thakali and M. Kitajima, *Sci. Total Environ.*, 2020, **737**, 140405.
- 42 P. A. Barril, L. A. Pianciola, M. Mazzeo, M. J. Ousset, M. V. Jaureguiberry, M. Alessandrello, G. Sánchez and J. M. Oteiza, *Sci. Total Environ.*, 2021, **756**, 144105.
- 43 S. E. Philo, E. K. Keim, R. Swanstrom, A. Q. W. Ong, E. A. Burnor, A. L. Kossik, J. C. Harrison, B. A. Demeke, N. A. Zhou, N. K. Beck, J. H. Shirai and J. S. Meschke, *Sci. Total Environ.*, 2021, **760**, 144215.
- 44 G. La Rosa, L. Bonadonna, L. Lucentini, S. Kenmoe and E. Suffredini, *Water Res.*, 2020, **179**, 115899.
- 45 S. Bofill-Mas and M. Rusiñol, *Curr. Opin. Environ. Sci. Health*, 2020, **16**, 7–13.
- 46 B. M. Pecson, E. Darby, C. N. Haas, Y. M. Amha, M. Bartolo, R. Danielson, Y. Dearborn, G. Di Giovanni, C. Ferguson and S. Fevig, *Environ. Sci.: Water Res. Technol.*, 2021, **7**, 504–520.
- 47 A. H. Chik, M. B. Glier, M. Servos, C. S. Mangat, X.-L. Pang, Y. Qiu, P. M. D'Aoust, J.-B. Burnet, R. Delatolla and S. Dorner, *J. Environ. Sci.*, 2021, **107**, 218–229.
- 48 A. D. George, D. Kaya, B. A. Layton, K. Bailey, S. Mansell, C. Kelly, K. J. Williamson and T. S. Radniecki, *Environ. Sci. Technol. Lett.*, 2022, **9**, 160–165.
- 49 M. Rafiee, S. Isazadeh, A. Mohseni-Bandpei, S. R. Mohebbi, M. Jahangiri-Rad, A. Eslami, H. Dabiri, K. Roostaei, M. Tanhaei and F. Amereh, *Sci. Total Environ.*, 2021, **790**, 148205.
- 50 S. Kim, L. C. Kennedy, M. K. Wolfe, C. S. Criddle, D. H. Duong, A. Topol, B. J. White, R. S. Kantor, K. L. Nelson and J. A. Steele, *Environ. Sci.: Water Res. Technol.*, 2022, (8), 757–770.
- 51 K. Bibby, A. Bivins, Z. Wu and D. North, *Water Res.*, 2021, 117438.
- 52 P. Foladori, F. Cutrupi, N. Segata, S. Manara, F. Pinto, F. Malpei, L. Bruni and G. La Rosa, *Sci. Total Environ.*, 2020, **743**, 140444.
- 53 W. Ahmed, P. M. Bertsch, K. Bibby, E. Haramoto, J. Hewitt, F. Huygens, P. Gyawali, A. Korajkic, S. Riddell and S. P. Sherchan, *Environ. Res.*, 2020, **191**, 110092.
- 54 P.-Y. Hong, A. T. Rachmadi, D. Mantilla-Calderon, M. Alkahtani, Y. M. Bashawri, H. Al Qarni, K. M. O'Reilly and J. Zhou, *Environ. Res.*, 2021, **195**, 110748.
- 55 Berlin\*, Berliner Wasserbetriebe - Water Usage at Home, <https://www.bwb.de/en/2266.php>, (accessed August 5, 2021).
- 56 H. M. Baalousha and O. K. Ouda, *Arabian J. Geosci.*, 2017, **10**, 1–12.
- 57 J. Tibbetts, *Combined sewer systems: down, dirty, and out of date*, National Institute of Environmental Health Sciences, 2005.
- 58 F. Wu, J. Zhang, A. Xiao, X. Gu, W. L. Lee, F. Armas, K. Kauffman, W. Hanage, M. Matus and N. Ghaeli, *mSystems*, 2020, **5**, e00614-20.
- 59 J. Schilling and J. Tränckner, *Water*, 2020, **12**, 628.
- 60 J. S. McClary-Gutierrez, Z. T. Aanderud, M. Al-Faliti, C. Duvallet, R. Gonzalez, J. Guzman, R. H. Holm, M. A. Jahne, R. S. Kantor and P. Katsivelis, *Environ. Sci.: Water Res. Technol.*, 2021, **7**, 1545–1551.
- 61 S. W. Olesen, M. Imakaev and C. Duvallet, *Water Res.*, 2021, **202**, 117433.
- 62 L. Zhang, L. Chen, X. Yu, C. Duvallet, S. Isazadeh, C. Dai, S. Park, K. Frois-Moniz, F. Duarte, C. Ratti, E. J. Alm and F. Ling, Microbial Species Abundance Distributions Guide Human Population Size Estimation from Sewage Microbiomes, bioRxiv, 2022, DOI: [10.1101/2020.12.15.390716](https://doi.org/10.1101/2020.12.15.390716).
- 63 S. Feng, A. Roguet, J. S. McClary-Gutierrez, R. J. Newton, N. Kloczko, J. G. Meiman and S. L. McLellan, *ACS ES&T Water*, 2021, **1**, 1955–1965.
- 64 M. Kitajima, H. P. Sassi and J. R. Torrey, *npj Clean Water*, 2018, **1**, 1–9.
- 65 A. Bivins, D. North, A. Ahmad, W. Ahmed, E. Alm, F. Been, P. Bhattacharya, L. Bijlsma, A. B. Boehm and J. Brown, *Wastewater-based epidemiology: global collaborative to maximize contributions in the fight against COVID-19*, ACS Publications, 2020.

